Linear and nonlinear optical spectroscopy of CdS nanoparticles in Nafion membranes

Emmanuel Bourdin, Fryod Z. Henari, Werner J. Blau, and John M. Kelly

Abstract — CdS nanoparticles embedded in Nafion membranes were studied by a variety of optical spectroscopic methods. Quantum confinement was achieved (particle mean diameter of 40 Å) and the growth was found to follow a linear temporal kinetic law. Discrete energy levels were observable, even at room temperature. They could be attributed to light hole and heavy hole 1S and 2S transitions. The experimental results are in good agreement with theoretical calculations of light hole and heavy hole masses in the cases of cubic CdS. An enhancement of the nonlinear susceptibility $\chi^{(3)}$ at the quantized exciton energy levels was observed. The clusters were found to be photo-unstable, with a diffusion-limited growth rate due to Ostwald ripening.

Keywords — optical spectroscopy, Nafion membranes, CdS nanoparticles.

Introduction

In the past decade, carrier confinement in semiconductors has attracted substantial interest, because of its technological importance and the interesting new phenomena and devices observable in such low dimensional structures. In this paper, we shall deal with materials confined in three dimensions, commonly referred to as quantum dots [1]. In that case, the energy levels are quantized and their optical response appears in the form of excitonic delta functions, with an enhanced oscillator strength. The semiconductor used is CdS. Confinement was achieved by embedding the material into an ionic exchange membrane with exceptionally well defined pore size, Nafion. Confinement effects were observed at room temperature in both linear absorption and luminescence spectroscopy. The nonlinear optical susceptibility $\chi^{(3)}$, is particularly sensitive to carrier confinement. Hence, its values were measured and showed a behaviour characteristic of a band-filling effect. The clusters, of different diameters, but still well confined after their formation, were found to aggregate following an Ostwald ripening processing over a period of days/weeks.

General background

Electronic structure

Simple quantum mechanics may be applied to determine the basic electronic structure of a quantum dot. We suppose that the particle radius, R, is much smaller than the exciton Bohr radius ($a_B = 28$ Å for CdS). The wave function is zero outside the particle, corresponding to an infinitely large potential barrier. Neglecting the Coulombic interaction of created electron-hole pairs, the wave function is of the following form [1, 2]:

$$\Psi_{n,l,m} = \Psi_{l,m}(\Theta,\phi)\frac{1}{R}\left\{\frac{2}{r}\right\}^{\frac{1}{2}} \frac{J_{l+\frac{1}{2}}(k_{nl}r)}{J_{l+\frac{3}{2}}(k_{nl}R)}, \quad (1)$$

where $\Psi_{l,m}$ are the normalized spherical functions; n is the principal quantum number, l is the momentum and J_x is a Bessel function. The quantities k_{nl} are defined by

$$J_{l+\frac{1}{2}}(k_{nl}R) = 0 \quad (2)$$

the roots of the Bessel function. Hence, k_{nl} may be written

$$k_{nl} = \Phi_{nl}/R. \quad (3)$$

For $l = 0$ we get from Eq.(2) that

$$k_{n0} = n\pi/R, \quad (4)$$

where $n = 1, 2, 3, \ldots$. For $l > 0$ the solutions are not simple, the first few being $\Phi_{0,1} = 3.14, \Phi_{1,1} = 4.49, \Phi_{2,1} = 5.76$ [3]. Using this wave function, Eq. (1) gives energy levels

$$E_{n,l} = E_g + \frac{h^2 k_{nl}^2}{8m_e\pi^2}. \quad (5)$$

This result leads to a series of discrete energy levels. For simplicity, the above treatment is formulated in terms of the conduction band states, but applies equally to the valence band. In considering transitions between conduction and valence states, the above equations will apply where m_e is replaced by the reduced mass $\mu = m_e m_h/(m_e + m_h)$, m_h being the hole effective mass. Because of the orthogonality of the wave functions, transitions are only allowed between states of the same quantum number; this condition, however, would be relaxed under more realistic conditions. The above treatment takes the most simplistic approach. The Coulomb interaction of a created electron-hole pair and polarization effects due to created charges should be included. As a first approximation, the 1S ($n = 0$, $l = 1$) wave function of the electron and hole can be used. Substituting into Schrödinger equation gives the energy for the lowest excited state as

$$E_{1S} = \frac{h^2}{8R^2}\left(\frac{1}{m_e} + \frac{1}{m_h}\right) - \frac{1.8\,e^2}{\varepsilon R} + polarization\ term. \quad (6)$$

The second term has to be replaced by $\frac{1.7e^2}{\varepsilon R}$ for the levels 1P and 1D [4]. If we can neglect the polarization term since it includes high order terms in $\frac{1}{R}$, then the Coulomb interaction (which actually corresponds to the exciton binding energy) can cancel the confinement term. In practice, the Coulombic term can be neglected for materials with a low band gap and a high dielectric constant, such as GaAs. But, higher band gap materials with large effective masses and smaller dielectric constant will show a cancellation of the electrostatic and quantum terms for one specific radius R_0. In the case of CdS, R_0 takes the value of 80 Å [4]. One more feature to consider is the fact that the valence energy levels are degenerate, leading to the well-known notions of light-hole and heavy-hole.

Nonlinear optical properties

Optical nonlinearlity in the band gap region of the semiconductors has attracted much attention due to large nonlinearities observed in this region [7]. Such nonlinearities are attractive, both from the point of view of the basic physics and for practical device applications in optical switching and signal processing. They mean that only low intensities and short device length are required, making an integrated miniaturized device technology possible.

Unlike in the bulk, where they are broad bands within which excitations could occur, now there are only single transitions separated by large gaps. Screening effects, whereby interactions are modified due to the presence of other charge carriers will be suppressed. A particular level may only be occupied by electrons of opposite spin, and so the exchange interaction is identically zero. The only mechanism which may operate in a true quantum dot is state filling and so for each spin the behaviour can be modelled as a simple two level saturable absorber. This implies that saturation will be achieved for one electron-hole pair per dot and that total saturation of the transition should be possible.

When semiconductors are confined, the stability of the excitons increases (the Coulombic interaction energy is much less than the separation between the quantum confined levels), and, as a consequence, its resonances are strongly enhanced and well resolved at room temperature.

It is possible to estimate the third-order nonlinear susceptibilityb $\chi^{(3)}$ from induced absorption changes $\Delta\alpha$ and refractive index Δn [5], we obtain then in a simple two level system:

$$\frac{\Delta\alpha}{I} = K_1 \left(\frac{a_B}{R}\right)^3 \operatorname{Im}\chi^{(3)} \text{ and } \frac{\Delta n}{I} = K_2 \left(\frac{a_B}{R}\right)^3 \operatorname{Re}\chi^{(3)}, \tag{7}$$

where I is the intensity inside the quantum dot and K_1 and K_2 are prefactors scaling the absorption and dispersion changes.

One can see immediately that large nonlinearities are expected when the confinement is such that the particles radius R is smaller than a_B.

There are several theories that have been proposed to predict the nonlinear optical behaviour of nanoparticles in the band gap region. Band-filling is the most likely effect and has been suggested by Roussignol et al. [6]. It arises from relaxation of free carriers to the band extrema before recombination. An analysis of this effect [7] predicts that

$$\chi^{(3)} \approx \frac{\alpha(\omega)}{\omega_o - \omega}, \tag{8}$$

where $\alpha(\omega)$ is the absorption at the wavelength corresponding to the frequency ω and $\frac{\hbar\omega_0}{2\pi}$ is the first excitation energy. A characteristic detuning factor will then appear at the resonance at an exciton energy level.

Others analyse the finite-size effects on the excitons in semiconductor microcrystallites [8]. The enhancement of the nonlinear polarizability originates from two conflicting concepts. One is due to the size quantization of excitons, this results in an enhancement factor of L^6 for $\chi^{(3)}$ per microcrystallites, i.e., an enhancement factor of L^3 for $\chi^{(3)}$ per unit volume. The other enhancement comes from deviation of the electronic excitation from an ideal harmonic oscillator. When the size of the microcrystallite is reduced, the latter effect increases while the former decreases.

The nonlinear optical polarizability is greatly modified for an assembly of semiconductor microcrystallites if the excitons in a single microcrystallite intereact strongly enough. It has been demonstrated [7] that $\chi^{(3)}$ vanishes when the interaction energy of two excitons is negligible in comparison with the off-resonance energy $(\omega - \omega_0)$. Under such conditions, excitons behave as harmonic oscillators, which do not show any nonlinear response. But under the opposite condition, we have an enhanced optical nonlinearity, and calculations give

$$\chi^{(3)} = K\frac{|p_{cv}|^4}{(\omega - \omega_0)^3}, \tag{9}$$

where K is constant depending on the geometry and size of the particles and p_{cv} is the transition dipole moment for the lowest excited states. Hence, from the wavelength dependence of the resonance behaviour, one can obtain in indication whichever effect may be dominant.

Fabrication of CdS in Nafion

Chemical preparation

The idealized pore/channel structure of Nafion is depicted in Fig. 1. Nafion 117 membranes (0.8 cm large, 3 cm long and 0.4 cm thick, furnished by Du Pont) were purified according to the following procedure. They were first stirred in boiling 0.2 M NaOH for two hours, then washed in Millipore water and ultrasonically treated with a 50% ethanol/50% water (in mass) mixture for 2.5 hours. Then, the membranes were treated with a 1M H_2SO_4 for one hour, finally the ultimate stage was a further ultrasonic treatment in Millipore water for 30 min. The incorporation of cadmium ions was achieved by soaking the membrane in an
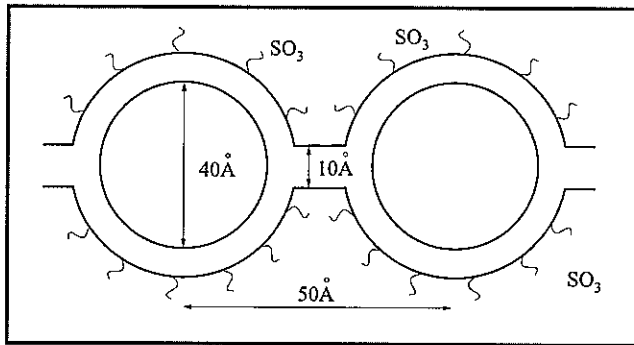
Fig. 1. Pore structure of Nafion membrane

appropriate volume of a 0.01 M cadmium sulphate solution for one hour. Two different exchange ratios (Cd^{2+} : Nafion) were used experimentally, namely 1:10 and 1:100. The samples were then dried at room atmosphere. The membranes were then mounted in a 1 ml quartz cell and exposed to dried hydrogen sulphide (atmospheric pressure) to convert them into the sulphide.

Transmission electronic microscopy

The microscopic morphology of the Nafion membranes will obviously dictate the cluster size and shape. Transmission electron microscopy shows a large number of particles, the largest having a diameter of around 800 Å. We do not observe a largely dispersed range of diameter from 40 to 800 Å, but two families of clusters. A small clusters family ($\emptyset \approx 40$ Å) and a mature and large clusters family ($\emptyset \approx 800$ Å), with some fluctuation (±20%) around those mean diameters. After 2 months of ageing, evidence of diffusion growth is clear. It can be noticed that clear regions, corresponding to a smaller density of clusters, are present around and beside the largest clusters, which suggests a diffusion of the small clusters that migrate towards the largest as described in the Ostwald ripening process: due to the moisture contained into the film, the smaller particles tend to dissolve in time, the solvated ions can then recrystallize on the larger semiconductor particles where they have a greater thermodynamic stability.

Optical spectroscopy

Linear absorption

Samples of Cd^{2+} membranes with different exchange ratios (1:10 and 1:100) were exposed to H_2S gas (atmospheric pressure) in a 5 ml quartz cell. The cell was mounted into the sample holder of a spectrophotometer (Phillips PYE UNICAM 8800). Their absorption spectra were recorded at different times of the CdS particles formation in the gas, this was carried at room temperature.

Figures 2 and 3 show the evolution of the absorption spectrum of the 1:100 and 1:10 exchange ratio samples, respectively. As can be seen, we have the formation of a shoulder in the bandtail of the absorption. This corresponds to the
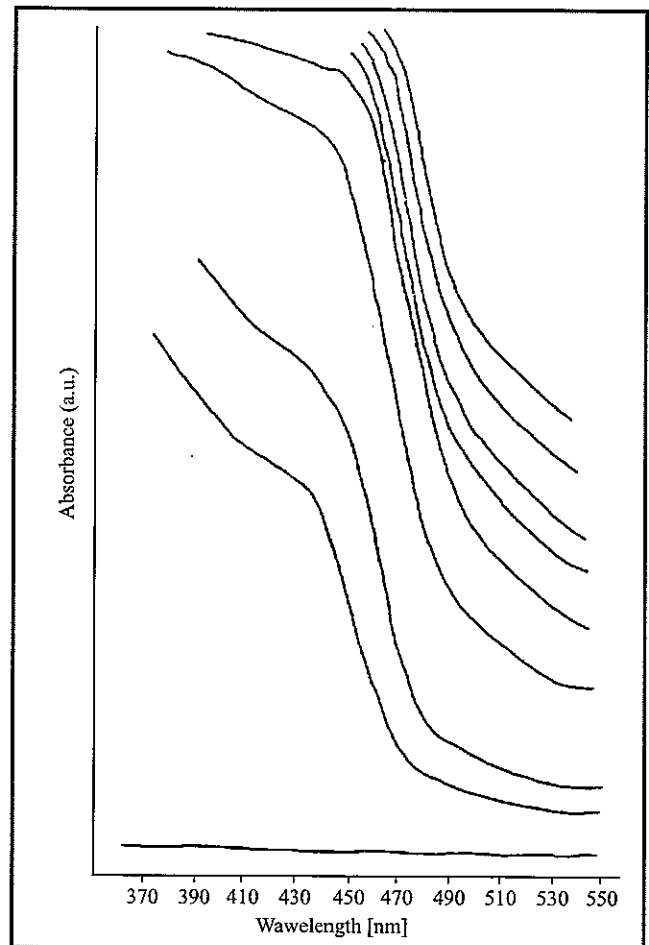

Fig. 2. Evolution of the absorption spectrum with time of exposure of a 1:10 exchange ratio Cd membrane exposed to dried hydrogen sulphide
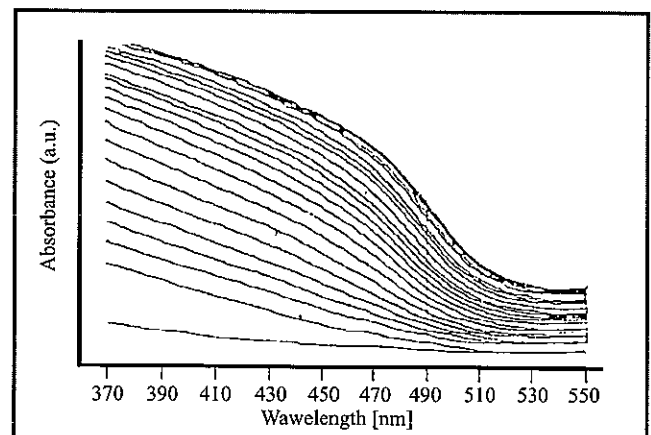

Fig. 3. Evolution of the absorption spectrum with time of exposure of a 1:100 exchange ratio Cd membrane exposed to dried hydrogen sulphide

The bottom curve corresponds to the absorption of the exchanged membrane just before exposure. The following curves, from bottom to top, correspond to different time of exposure with a 1 minute step up to 15 minutes of exposure, then the absorption was recorded every ten minutes until a final exposure of 50 minutes.

first transition 1S denoted before. As the growth of the particles goes on, the band edge of the absorption is found to be red-shifted, which corresponds to the decrease of the confinement factor. The 1S transition energy was calculated at the tip of the shoulder. Using the Eq. (6) we can calculate the radius of the particle.

Figure 4 shows the plot of diameter versus reaction time. For both samples, we obtain a linear kinetic growth law. As expected, the 1:10 sample shows larger particles (mean
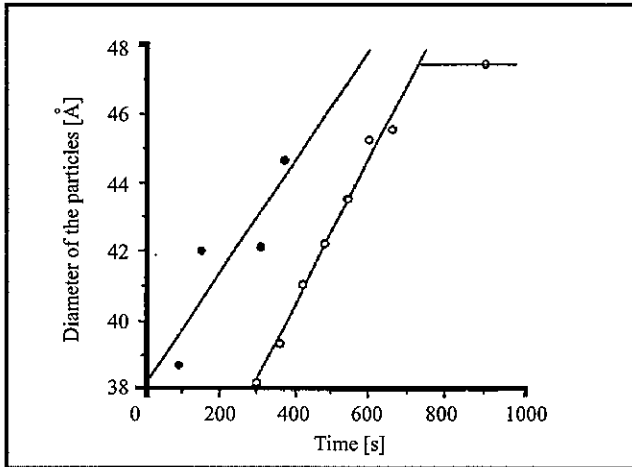

Fig. 4. A linear kinetic law is obtained for the growth of the nanoparticles
The black circles stand for the 1:10 exchange ratio sample and the white circles for the 1:100 exchange ratio sample.

initial diameter = 39 Å) than the 1:100 sample (mean initial diameter = 32 Å), but they both have approximately the same growth rate, which is around 1 Å/45 s. A saturation state is reached after 15 minutes for the case of the 1:100 sample. We attribute this to the fact that there are no more Cd^{2+} sites available for the reaction. The stabilization of the band gap is associated with the saturation of the absorption coefficient, indicating clearly that the growth has stopped for a mean diameter of approx. 50 Å.

Those values are very much in agreement with previous measurements made with ferric ions clusters in Nafion membranes [9]. It was found that the ions are present under two species: clusters of variable sizes or monomeric /dimeric species bridged by oxygen or hydroxyl ions. In this case, the mean diameter of the clusters was also ≈ 40 Å. A large proportion of dimers could also be observed, the concentration depending on the solution and the drying procedure.

If all the Cd^{2+} ions were in the clusters, then we should have ratio of $\left(\frac{1:10 \text{ mean radius}}{1:100 \text{ mean radius}}\right)^3 = \frac{1:10}{1:100} = 10$. In fact, we found a value of 1.8. This reflects the importance of the dimeric form of the ions in the membrane. Those smaller units are present in the channels in between the clusters, and have been reported to be responsible for the ion transport through the membrane [9]. In that case, it is obvious that the fraction of such dimers is more important in the 1:10 sample than in the 1:100 sample. We shall discuss their importance later on.

Luminescence excitation

The luminescence spectra were recorded with a PERKIN-ELMER MPF-44 B fluorescence spectrophotometer at room temperature. The excitation wavelength was chosen to be 450 nm, 2.76 eV, i.e. well above the band gap. The results obtained for a 1:10 exchange ratio are shown in Fig. 5. At the early stage of the reaction, we can distin-
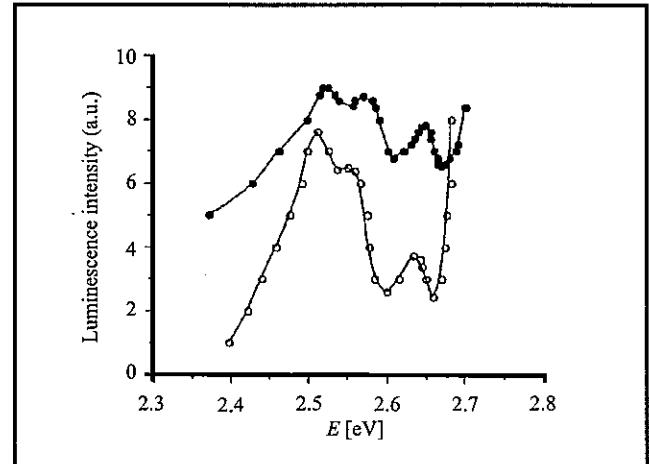

Fig. 5. Luminescence spectrum of a 1:10 exchange ratio membrane
White circles curve after 2 minutes and black circles curve after 5 minutes of exposure to dried hydrogen sulphide. The excitation wavelength is 450 nm (2.76 eV).

guish 3 sharp peaks at 2.52 eV, 2.57 eV and 2.65 eV. The fact that there are not equidistant shows that we cannot attribute them to phonons interaction. They can, however, be assigned to the confinement of the energy levels, since the mean diameter measured in the former section is 40 Å. We attribute the peaks at 2.52 eV, 2.57 eV and 2.65 eV respectively to the transitions $E_{1S,HH}$, $E_{1S,LH}$ and $E_{1P,HH}$. We have:

$$E_{1S,HH} = E_g + \frac{h^2}{8R^2}\left(\frac{1}{m_e} + \frac{1}{m_{HH}}\right) - E_{b.exc.} \qquad (10)$$

$$E_{1S,LH} = E_g + \frac{h^2}{8R^2}\left(\frac{1}{m_e} + \frac{1}{m_{LH}}\right) - E_{b.exc.}, \qquad (11)$$

$$E_{1P,HH} = E_g + \frac{h^2}{8R^2}\left(\frac{4.49}{\pi}\right)^2\left(\frac{1}{m_e} + \frac{1}{m_{HH}}\right) - E_{b.exc.} \qquad (12)$$

Two facts support the attribution of the peaks. First of all, we can calculate the values of the m_{HH} and m_{LH}. The effective mass of the electron m_e has been reported to be in between 0.16 m_0 in CdS bulk samples [10,11]. The masses of the heavy hole and the light hole are given by [12]

$$m_{HH} = \frac{m_0}{\gamma_1 - 2\gamma_2}, \qquad (13)$$

$$m_{LH} = \frac{m_0}{\gamma_1 + 2\gamma_2},\qquad(14)$$

where γ_1 and γ_2 are the Luttinger parameters of the valence band. In the case of cubic CdS, the literature values give [10]

$$m_{HH} = 0.94\,m_0 \quad \text{and} \quad m_{LH} = 0.16\,m_0\,.$$

First, let us assume that the exciton binding energy is not too important. Then, using the data of $m_{HH} = 0.94\,m_0$ and $m_e = (0.18 \pm 0.02)\,m_0$, and the experimental data shown in Table 1 for the peaks values, we find $m_{LH} = 0.1\,m_0$.

Table 1
Evolution of the energy levels as the particles grow

Time after the begining of the reaction	$E_{1S,HH}$ [eV]	$E_{1S,LH}$ [eV]	$E_{1P,HH}$ [eV]	α	
				$E_{exc} = 0$	E_{exc} for the cancellation at 80Å
2 min	2.52	2.57	2.65	0.43	0.47
5 min	2.51	2.55	2.63	0.43	0.5
5 hours	2.46				
1 day	2.42				

In order to take into account the exciton binding energy, we use the fact that the value of the radius for which we see a cancellation of the electrostatic and quantum terms is 80 Å and we can take a value of 40 Å for the diameter of the particles after 2 minutes. We then arrive to the following results $m_{LH} = (0.15 \pm 0.01)\,m_0$. Those results are very much in agreement with the theory thus supporting the attribution of the peaks made before. Secondly, assuming that the binding energy of the exciton is the same in both states 1S and 1P and can be neglected, compared to the confinement term, then it follows that the ratio α

$$\alpha = \frac{E_{1S,HH}-E_g+E_{exc.}}{E_{1P,HH}-E_g+E_{exc.}} = \left(\frac{4.49}{\pi}\right)^{-2} = 0.49\,.\qquad(15)$$

Experimental data of that ratio are given in Table 1. We find a value of 0.43 which is slightly lower than 0.49. It is obvious that this discrepancy comes from the assumptions made earlier. As before, in order to take into account the exciton binding energy, we use the fact that the value of the radius for which we see a cancellation of the electrostatic and quantum terms is 80 Å and we take a value of 40 Å for the diameter of the particles after 2 minutes and 5 minutes. We then arrive to a value of 0.47 (after 2 min) and 0.5 (after 5 min). Once again, those values support the attribution given to the peaks.

The attribution of the peaks is strongly supported by the values of the ratio α definited in Eq. (15).

As the growth goes on, the small sharp peaks shift towards lower energies and the fine and discrete structure disappears, this is due to the growth of the particles and the decrease of the confinement term, associated with a hybrid molecular-semiconductor structure of the clusters.

Another aspect to consider is the relative importance of the different intensity of the peaks. At the early stages of the reaction, they all have approximately the same intensity, indicating well separated energy levels, i.e. each band is quickly filled up and one has a carrier recombination at every levels. However, as the growth proceeds, it becomes clear that the 1S,HH transition becomes predominant. This is expected, since as the particles grows, we tend more towards a quasi-bulk structure which is characterized with only one recombination peak occurring at the bottom of the conduction band.

Figure 6 shows the ageing effect on the particles. A general remark on the data is that after five hours in room atmosphere, the excitation peak value is still larger than 2.42 eV, indicating then that the confinement term is dominating the Coulombic term, which means that the mean radius of the cluster is less than 80 Å.
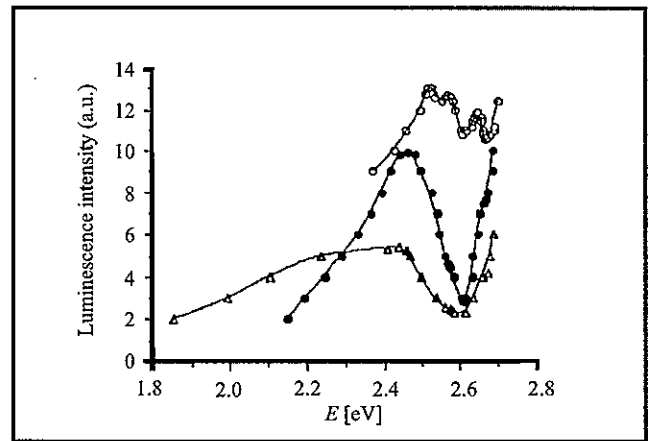

*Fig. 6.* Ageing effect on the luminescence spectrum of a 1:10 exchange ratio membrane
White circles curve after 2 min of exposure to dried hydrogen sulphide, black circles curve after 5 hours of storage at room atmosphere, and triangle curve after 1 day of storage at room atmosphere. The excitation wavelength is 450 nm (2.76 eV).

Several further features were observed in the luminescence spectra. A small peak at 825 nm (1.51 eV) is present in every case. This is explain by the following reaction where oxygen acts as a donor:

$$1/2\,O_2 \Longleftrightarrow CdO + V_{Cd^{2-}} + 2h^+$$
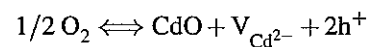
which predicts a peak at 820 nm.
After storage at room atmosphere a large excitation peak is found to appear at 700 nm (1.78 eV) which was attributed to Sulphur vacancies

$$h^+ + V_S \longrightarrow V_{S+} + h\nu$$
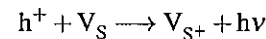
and ionised vacancies are subsequently refilled by conduction band electrons produced concomitantly with h^+ by band gap excitation.
Finally, the effect of ageing on the samples was to, firstly shift the peak value to lower energy, and subsequently, decrease its intensity. The first point is reflecting the fact

that the particles keep on growing, even in the absence of H$_2$S gas. This is due to the presence of moisture in the membranes, which contains dilute form of the H$_2$S, and which helps the migration of the cadmium ions within the channels. These ions then react at the surface of the clusters, causing then an enlargement of them according to the following reaction:

$$(CdS)_n + Cd^{2+}_{solv} + S^{2-}_{solv} \Longleftrightarrow (CdS)_{n+1}$$
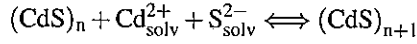
The fact that the intensity decreases is analysed as showing the quenching by surface defects, appearing during that diffusion-limited growth phase.

Nonlinear optical properties

Two methods are used to investigate the nonlinear response of these systems. As discussed in section *Nonlinear optical properties*, semiconductor quantum dots should show saturable absorption. Therefore, the intensity dependence of the transmission must be investigated. A laser induced grating, i.e. degenerate four-wave mixing set-up was used to measure the magnitude and dispersion of $\chi^{(3)}$ [13].
Maximal nonlinear response is expected when the excitation wavelength is in resonance with the quantized transitions. Since this depends on the particle dimensions, a tunable laser source is required. In all experiments described below, a Molectron DL-100 dye laser, pumped by a low pressure Molectron UV-300 N$_2$ laser, was employed giving pulses of 5 ns duration and typically 30 μJ energy.

Nonlinear absorption

Two types of samples with different emission spectra but the same 1:10 exchange ratio were studied. One had an maximal emission peak at 500 nm and the second one had an emission maximum at 700 nm. Although the signal was found to slightly decrease along the experiment (a couple of percent in 2–3 hours), some general trends can be deduced. The experimental set-up was as follows: The output of the dye laser was focused onto the samples. The input and transmitted energy were measured using calibrated silicon photodiodes, a fraction of the input being split-off with a beamsplitter. The input intensity could be varied using neutral density filters to attenuate the energy per pulse. The beam waist at the sample was measured with calibrated pinhole apertures to determine the intensity.
For small initial absorption ($T_0 > 0.1$), the transmission versus the input intensity will the follow equation

$$T = T_0 \quad 1 / \left(1 + \frac{I}{I_{sat}}\right). \quad (16)$$

Here, I_{sat} is the saturation intensity and, for a two-level system, is given by

$$I_{sat} = \frac{h\nu}{2\sigma_0\tau}, \quad (17)$$

where σ_0 is the carrier absorption cross-section (10-17 cm^2 for CdS) and τ is the excited state lifetime of the carriers. Figure 7 shows the results obtained for the 700 nm emission peak sample. No major difference was found between both samples, they both had a saturation intensity of (2.5 $\pm$0.5) 10^{11} W/cm^2 and an extremely short, calculated lifetime of 1 ps (at a wavelength of 446 nm). Saturation ($T_{(I \to \infty)} \to 1$)
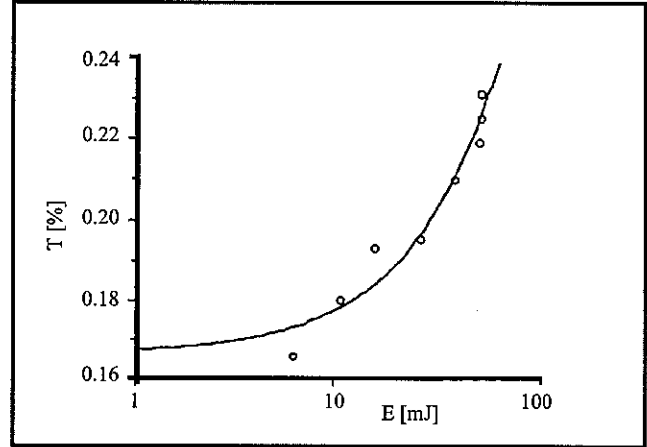

Fig. 7. Pulse energy dependent bleaching of the sample transmission $T = \exp(-\alpha l)$, and hence absorption saturation for a CdS Nafion membrane (exchange ratio of 1:10) with an emission peak at 700 nm
The solid line represents a fit to Eq. (13).

did not occur completely which demonstrates a sizeable non-saturable absorption which may be either due to excited free carrier absorption and/or non-saturable background absorption due to extremely fast relaxing species.

Degenerate four-wave mixing

To produce a laser induced grating, two coherent beams must be made to interfere. The output from the dye laser was collimated and brought around the table into a 50/50 cubic beam splitter. To achieve temporal overlap of the pulses a delay line was introduced on one arm; this proved especially necessary because of the very short coherence length of the pulses. The two collinear beams were brought to a focus and overlap by either a 30 or 50 cm focal length lens. When a material with a suitable nonlinear response was introduced into the overlap region, self-diffraction will occur. This may be observed by monitoring the beams on the opposite side of the sample. Two bright spots will be seen, corresponding to the straight through beams. To either side, fainter spots appear corresponding to the diffracted beams. For highly nonlinear materials, several diffracted orders may be observed. When measuring the magnitude of the diffracted beam, the signal obtained with the nearer pump beam blocked was also measured, and subtracted from the diffracted signal. This removes the component due to background scatter and it also ensures that only a transient grating is measured. Permanent gratings may also be written by physical damage to a material, or by other photochemical effects.

Degenerate four-wave mixing theory was used to calculate the magnitude of the effective third-order susceptibility, $|\chi^{(3)}|$. The self diffraction effect may be viewed as forward four-wave mixing where the probe beam is equal to and collinear with one of the pump beams. For this geometry $|\chi^{(3)}|$ can be calculated [14]:

$$|\chi^{(3)}| = \frac{8c^2n^2\varepsilon_0\alpha\sqrt{\eta}}{3\omega I_1(1-T)}, \qquad (18)$$

where c is the speed of light, n-the linear refractive index, α-the linear absorption, ω-the frequency, I_1-the pump intensity, and T-the transmission at I_1. It should be noted that the diffraction intensity depends quadratically, and thus the diffracted signal cubically, on the incident intensity I_1, as expected for a third-order nonlinear process.

The results of the intensity dependence of $|\chi^{(3)}|$ are shown in Fig. 8. They show within experimental accuracy ($\pm 20\%$
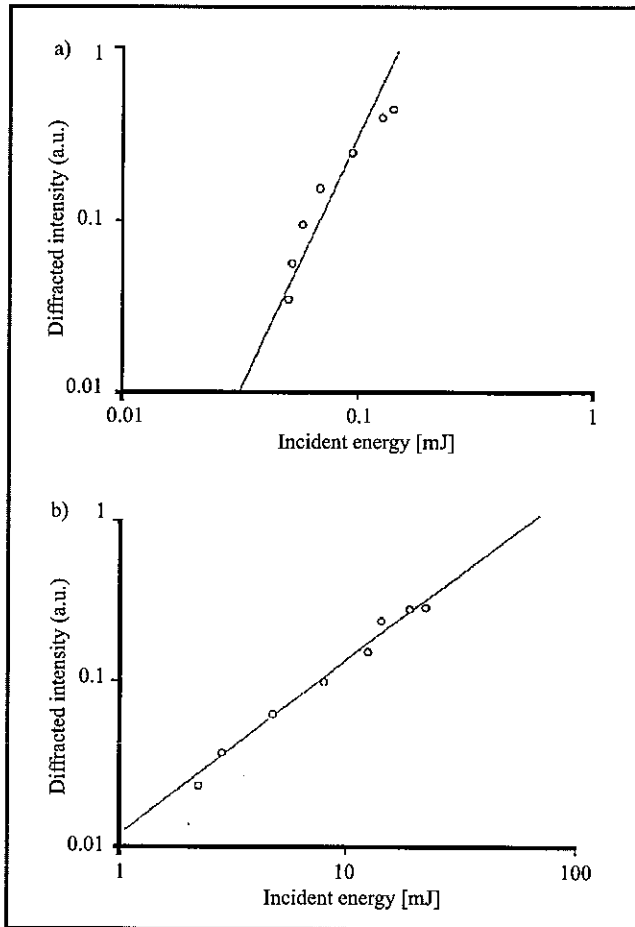

Fig. 8. Dependence of the diffracted intensity in the degenerate four-wave mixing experiment on incident pulse energy (proportional to intensity) for a CdS Nafion sample: a) exchange ratio of 1:10 - emission peak at 500 nm; the straight line corresponds to a slope of 3; b) exchange ratio of 1:10 - emission peak at 700 nm. The straight line corresponds to a slope of 1.

of intensity) that a third-order process occurs in the first sample, whereas we obtain a perfectly linear behaviour in the case of the second sample. This corresponds to

a quenching of the third-order process which is identical to the effect observed as 'photo-darkening' in doped glasses [1, 6], and is due to the presence of traps in the middle of the band gap, attributes to the 700 nm emission peak.

As discussed above in section *Nonlinear optical properties*, the wavelength dependence of the third-nonlinear susceptibility $\chi^{(3)}$ should give an indication of the process going on in each of both samples. It is expected that this should get enhanced at wavelengths in resonance with an exciton energy level.

Such a detuning effects can be seen in Fig. 9. Enhancement occurs when the exciton interaction is larger than off-resonance energy. If the band-filling theory applies [7]:

$$|\chi^{(3)}| = \frac{M\,\alpha(\omega)}{\omega_{g1} - \omega} + \frac{N\,\alpha(\omega)}{\omega - \omega_{g2}}, \qquad (19)$$

which yields $\omega_{g1} = 2.89$ eV and $\omega_{g2} = 2.72$ eV, M and N being two fitting constants. None of the other effects outlined in section *Nonlinear optical properties* give a satisfactory alternative fit. We believe that band filling depicts the physical reality quite well since we have a hybrid band structure, i.e. we have indeed a discrete repartition of quite broad bands. From the experiments presented, it is not
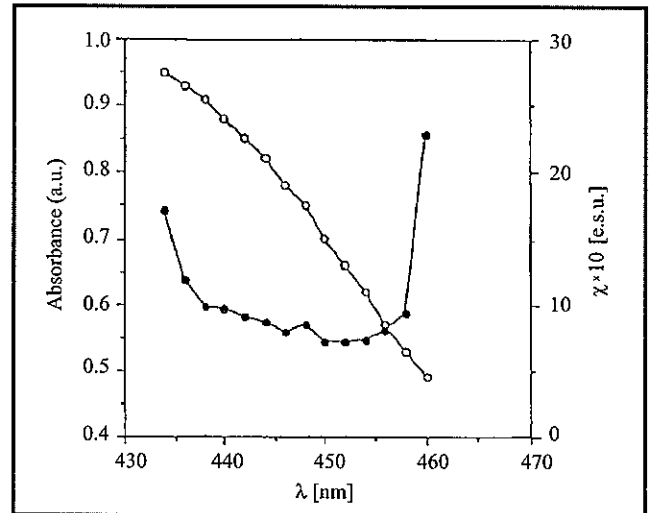

Fig. 9. The third nonlinear susceptibility $\chi^{(3)}$ (full circles) and absorption spectra (open circles) of a CdS Nafion sample (exchange ratio of 1:10 - emission peak at 500 nm).

possible to conclude what energy levels exactly correspond to the two observed resonances. 2.89 eV and 2.72 eV might correspond to two different diameter particles (one in Nafion cluster of 40 Å, and one located in the channel with diameter of 10 Å), or alternatively two consecutive exciton energy levels.

The magnitude of $|\chi^{(3)}|$ measured was very sizeable with an off-resonance value is $6 \cdot 10^{-9}$ esu and a resonance enhancing factor of at least 10. Those results are well in accordance with previous results reported by Hayashi et al. [16]. In their case, CdS particles embedded in acrylonitrile - styrene copolymer films with diameter ranging from 3 to 5 nm were studied. The ratio of nonlinearity to absorption

coefficient, which represents some kind of 'figure-of-merit' of the nonlinear material, was found to be $9 \cdot 10^{-10}$ esu/cm. This is comparable to a value of 8-10-10 esu/cm observed in the experiments reported here. An enhancement of the ratio $\frac{\chi^{(3)}}{\alpha}$ by one order of magnitude was observed near the exciton shoulder in the absorption spectrum, similar to our results.

Time resolved measurements were made by delaying one of the excitation beams with respect. The temporal resolution gives information about the speed of the nonlinear response of the samples and with incoherent pulses such as the ones applied here, in particular, about the dephasing time [17]. The temporal width (FWHM) of the peak was 3 ps which corresponds to the coherence time rather than to the width of the laser pulse. This indicates that the dephasing time is considerably faster than ≈ 1 ps. The excited state lifetime of 1 ps derived from the saturation measurements presented in section *Nonlinear absorption* also agree well with a reported relaxation time of 1.3 ps in similar samples [18].

Conclusions

Small clusers of CdS have been prepared in Nafion and their optical properties have been characterized. The kinetics of particle growth in H_2S gas was found to be linear in time. The diameter of the clusters was found to increase with time, and this is linked to the presence of moisture within the film. Exciton peaks were observed at room temperature in absorption and emission, and their attribution fits well with available data. Nonlinear measurements are very encouraging and clearly show an enhancement of the discrete energies of the excitons. The results show clusters with a mean diameter of approx. 40 Å and a hybrid band like structure.

Acknowledgements

References

[1] P. Horan and W. Blau, *Phase Trans.*, vol. 24–26, p. 605, 1990.

[2] Al. Efros and A. L. Efros, *Sov. Phys. Semicond.*, vol. 16, p. 775, 1982.

[3] S. Flügge, *Practical Quantum Mechanics*. Berlin: Springer-Verlag, 1971.

[4] L. Brus, *IEEE J. Quant. Electron.*, vol. QE-22, no. 9, p. 1909, 1986.

[5] G. A. Ozin, S. Kirby, M. Meszaros, S. Ozkar, A. Stein, and G. D. Stucky, in *Materials for Nonlinear Optics: Chemical Perspectives* (ACS Symposium Ser. 455, Boston, Massachussetts, April 1990), p. 554.

[6] P. Roussignol, D. Ricard, J. Lukasik, and C. Flytzanis, *J. Opt. Soc. Am. B*, vol. 4, no. 5, 1987.

[7] B. S. Wherrett and N. A. Higgins, *Proc. Roy. Soc. London Ser. A*, vol. 379, p. 67, 1982.

[8] E. Hanamura, *Phys. Rev. B*, vol. 37, no. 3, p. 1273, 1988.

[9] C. Heitner-Wirguin, E. R. Bauminger, F. Labensky de Kanter, and S. Ofer, *Polymer*, vol. 21, p. 1327, 1980.

[10] S. V. Nair, L. M. Ramaniah, and K. C. Rustagi, *Phys. Rev. Lett.*, vol. 68, no. 6, p. 893, 1992.

[11] K. I. Kang, B. P. McGinnis, Sandalphon, Y. Z. Hu, S. W. Koch, N. Peyghambarian, A. Mysyrowicz, L. C. Liu, and S. H. Risbud, *Phys. Rev. B*, vol. 45, no. 7, p. 3465, 1992.

[12] C. Weisbush and B. Vinter, *Quantum Semiconductor Structure*. New York: Academic Press, 1991.

[13] H. E. Eichler, P. Günter, and D. W. Pohl, *Laser Induced Dynamic Gratings*. Berlin: Springer Verlag, 1986.

[14] R. C. Caro and M. C. Gower, *IEEE J. Quant. Electron.*, vol. QE-18, p. 1376, 1982.

[15] A. I. Ekimov and A. A. Onushchenko, *J. Opt. Soc. Am. B*, vol. 10, no. 1, p. 100, 1993.

[16] T. Hayashi *et al.*, in *Organic Materials for Non-linear Optics III* (Royal Society of Chemistry, Oxford, 1992), p. 197.

[17] K. Misawa, T. Hattori, T. Kobayashi, Y. Ohashi, and H. Itoh, *Springer Proc. Phys.*, vol. 36, p. 66, 1989.

[18] T. Kobayashi, S. Nomura, and K. Misawa, *Proc. SPIE*, vol. 1216, p. 105, 1990.

Emmanuel Bourdin, Fryod Z. Henari, Werner J. Blau,
Department of Physics,
John M. Kelly,
Department of Chemistry
Trinity College Dublin, Dublin 2, Ireland